

# Ethanol Assisted Transfer for Clean Assembly of 2D Building Blocks and Suspended Structures

Xin Yang, Xiuqiang Li, Yu Deng, Yuxi Wang, Guoliang Liu, Cong Wei, Hai Li, Zhen Wu, Qinghui Zheng, Zhiwen Chen, Qing Jiang, Haiming Lu,\* and Jia Zhu\*

As two dimensional materials (2D materials) demonstrate unique and diverse properties, clean transfer methods can serve a cornerstone for creative assembly of these 2D building blocks for both fundamental explorations and versatile applications. One of the major challenges for preserving the pristine properties of 2D materials during transfer and construction is to debond 2D materials from original substrates without inducing structural damage and external contamination. In this work, through both molecular dynamic studies and experimental demonstration, it is found that droplets of ethanol, a common and environmental friendly solvent, can be used to effectively reduce the adhesion energy between 2D materials and substrates, and therefore enable a clean transfer method for 2D materials. Various assembled structures based on 2D building blocks, such as van der Waals heterostructures, predesigned artificial patterns, 2D materials on suspended devices are all demonstrated. Thermal conductivity measurements of MoS<sub>2</sub> nanosheets on a suspended microbridge device also confirm the successful application of suspended 2D transfer. It is expected that this ethanol assisted transfer method can enable clean assembly of 2D building blocks for construction of novel structures and suspended devices.

## 1. Introduction

Two dimensional materials (2D materials) have received a tremendous amount of attention in the community of material sciences for their unique properties<sup>[1]</sup> such as versatile band structures,<sup>[2]</sup> high carrier mobility,<sup>[3]</sup> tunable photoelectric properties,<sup>[4]</sup> high catalytic activity,<sup>[5]</sup> and so on. These 2D building blocks also enable the construction of various novel structures such as van der Waals heterostructures (vdWHs)<sup>[6]</sup> with new properties and functionalities.<sup>[7]</sup> In the past few years, several methods have been developed for transfer and integration of 2D materials into functional structures.<sup>[8]</sup> Techniques such as polymer layers<sup>[9]</sup> assisted wet transfer,<sup>[7,10]</sup> dry transfer<sup>[11]</sup> by hot pressing,<sup>[12]</sup> wet-contact printing method,<sup>[13]</sup> wedging transfer<sup>[14]</sup> have been heavily employed in the investigations of 2D building blocks. However, several issues that often occur during the transfer stage, such as self-damage or

contaminates like polymer residues,<sup>[15]</sup> need to be addressed. Especially for the construction of suspended structures, quite often they would either cause performance degradation,<sup>[15]</sup> or the destruction of fragile device.<sup>[16]</sup> It is crucial that a clean, feasible, and precise transferring method that overcomes these issues is developed so that the investigation of the 2D world can progress undeterred. One of the fundamental challenges for transferring 2D materials is detaching the 2D materials from the original substrate without damaging it or introducing contamination. Through both molecular dynamic study and experimentation, we would like to demonstrate that ethanol can effectively reduce the adhesion energy between 2D materials and their substrates, allowing 2D materials to be detached from the original substrate feasibly without causing damage to the material or introducing contamination. After that, the manipulation of needle with target sample will be achieved onto suspended device successfully without destruction to fragile device.

## 2. Results and Discussion

We first perform the molecular dynamic (MD) study (Figure S1, Supporting Information) to examine the effect of ethanol on the adhesion energy between 2D materials and a substrate.

X. Yang, X. Li, Y. Deng, Y. Wang, G. Liu, Z. Wu, Q. Zheng,  
Prof. H. Lu, Prof. J. Zhu  
National Laboratory of Solid State Microstructures  
College of Engineering and Applied Sciences  
Jiangsu Key Laboratory of Artificial Functional Materials  
Nanjing University  
Nanjing 210093, P. R. China  
E-mail: haimlu@nju.edu.cn; jiazhu@nju.edu.cn

C. Wei, Prof. H. Li  
Key Laboratory of Flexible Electronics (KLOFE)  
and Institute of Advanced Materials (IAM)  
Jiangsu National Synergetic Innovation Center  
for Advanced Materials (SICAM)  
Nanjing Tech University (NanjingTech)  
30 South Puzhu Road, Nanjing 211816, P. R. China

Z. Chen, Q. Jiang  
Key Laboratory of Automobile Materials  
Ministry of Education  
School of Materials Science and Engineering  
Jilin University  
Changchun 130022, P. R. China

 The ORCID identification number(s) for the author(s) of this article can be found under <https://doi.org/10.1002/adfm.201902427>.

DOI: 10.1002/adfm.201902427

**Table 1.** Different systems and their Gibbs free energy after adding ethanol for MoS<sub>2</sub>.

System	Gibbs free energy [kcal mol <sup>-1</sup> ]	ΔG [kcal mol <sup>-1</sup> ]
C <sub>2</sub> H <sub>6</sub> O–MoS <sub>2</sub> –SiO <sub>2</sub>	35 795.33	
MoS <sub>2</sub> –C <sub>2</sub> H <sub>6</sub> O–SiO <sub>2</sub>	35 679.92	–115.41
C <sub>2</sub> H <sub>6</sub> O–10MoS <sub>2</sub> –SiO <sub>2</sub>	161 319.49	
10MoS <sub>2</sub> –C <sub>2</sub> H <sub>6</sub> O–SiO <sub>2</sub>	161 205.32	–114.17

MoS<sub>2</sub>, one of the most heavily investigated 2D materials, is used as our first example. It can be found that the Gibbs free energy of ethanol between MoS<sub>2</sub> and SiO<sub>2</sub> substrate (as in MoS<sub>2</sub>–C<sub>2</sub>H<sub>6</sub>O–SiO<sub>2</sub> in Table 1) is lower than that of ethanol on top of MoS<sub>2</sub> (as in C<sub>2</sub>H<sub>6</sub>O–MoS<sub>2</sub>–SiO<sub>2</sub> in Table 1) for both single layer and ten layer MoS<sub>2</sub>. The reason for lower energy when intercalating ethanol between MoS<sub>2</sub> and vitreous SiO<sub>2</sub> should mainly result from the replacement of solid–solid MoS<sub>2</sub>–SiO<sub>2</sub> interface by solid–liquid C<sub>2</sub>H<sub>6</sub>O–SiO<sub>2</sub> interface, since the free energy of solid–liquid interface is usually smaller than that of solid–solid interface.<sup>[17]</sup> The present work allows an estimate of the energy of adhesion between MoS<sub>2</sub> and SiO<sub>2</sub> or C<sub>2</sub>H<sub>6</sub>O as  $E_{\text{adh}} = E(\text{SiO}_2 \text{ or } \text{C}_2\text{H}_6\text{O}) + E(\text{MoS}_2) - E(\text{MoS}_2 + \text{SiO}_2 \text{ or } \text{C}_2\text{H}_6\text{O})$ , where  $E$  is the total energy after geometry relaxation. As shown in Table 2, the adhesion energy is –96.35 kcal mol<sup>-1</sup> between MoS<sub>2</sub> and SiO<sub>2</sub>. Once the ethanol is inserted between MoS<sub>2</sub> and SiO<sub>2</sub>, the adhesion energy between the MoS<sub>2</sub> and the ethanol is –72.30 kcal mol<sup>-1</sup>, which is weaker than that between MoS<sub>2</sub> and SiO<sub>2</sub>. Therefore, lower Gibbs free energy of the system and weaker adhesion energy between the MoS<sub>2</sub> and the ethanol make the ethanol solution spontaneous intercalate between MoS<sub>2</sub> and SiO<sub>2</sub> and facilitate the detachment

**Table 2.** Different systems and their adhesion energy before and after adding ethanol for MoS<sub>2</sub>.

System	Adhesion energy [kcal mol <sup>-1</sup> ]	Reduction ratio
MoS <sub>2</sub> –SiO <sub>2</sub>	–85.23	
MoS <sub>2</sub> –C <sub>2</sub> H <sub>6</sub> O	–63.47	34.28%
10MoS <sub>2</sub> –SiO <sub>2</sub>	–96.35	
10MoS <sub>2</sub> –C <sub>2</sub> H <sub>6</sub> O	–72.30	33.26%

of the 2D materials from the original substrate. Moreover, in order to further describe the effect of ethanol on the adhesion energy between 2D materials and a substrate and verify of the results from MD calculations, we performed a series of density functional theory calculations and they show the same effect of ethanol as that illustrated in MD simulation (Figure S2, Table S3, Supporting Information). More details about these two simulation methods are available in the Supporting Information. What is more exciting is this MD study can be generalized to other material systems such as graphene, as shown in Tables S1 and S2 of the Supporting Information. At the same time, ethanol intercalation has also been confirmed by performing atomic force microscope (AFM) in liquid ethanol (Figure S3, Supporting Information). The thickness of MoS<sub>2</sub> sample tested in ethanol solution is 8.48 nm, thicker than that in air (5.36 nm), which provides a direct proof of ethanol intercalation.

The reduced adhesion energy between 2D materials and the substrate makes a clean and precise transfer possible. Figure 1 shows the schematic explaining the process for transferring 2D material from the original substrate to a target one. A control table including an optical microscope and a micromanipulator

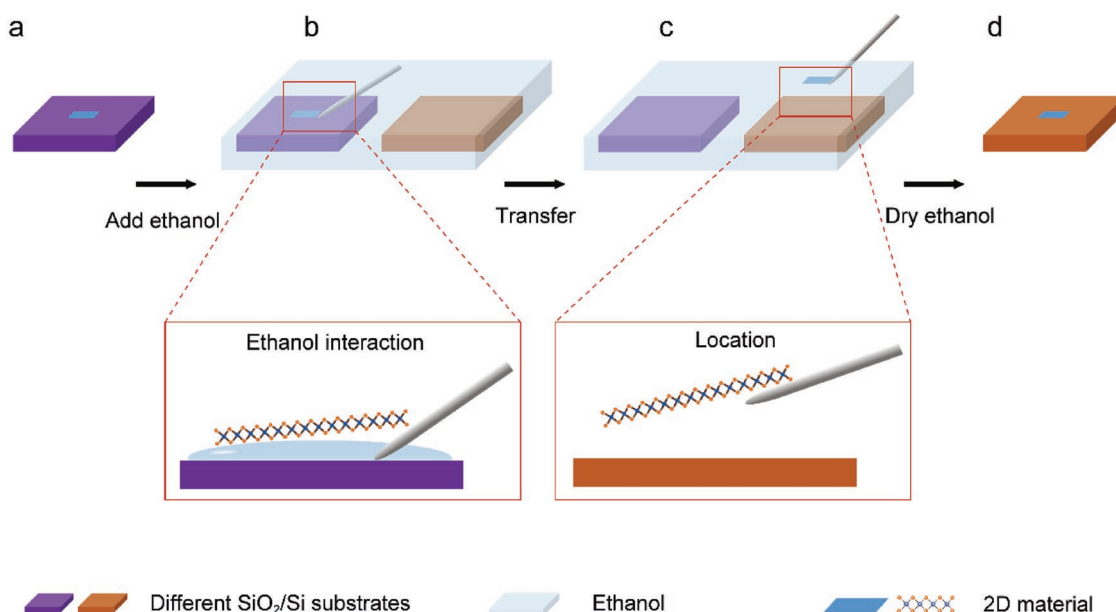


**Figure 1.** Schematic illustration of clean and precise transfer of 2D material. a) 2D material on a 300 nm SiO<sub>2</sub>/Si substrate. b) The solution intercalates into the space between the 2D material and the substrate after adding ethanol, then we can easily pry up the sample. c) Controlling the probe with a micromanipulator to transfer the sample in ethanol and locate the sample to target position. d) Drying the ethanol, then the sample is finally transferred onto another substrate.

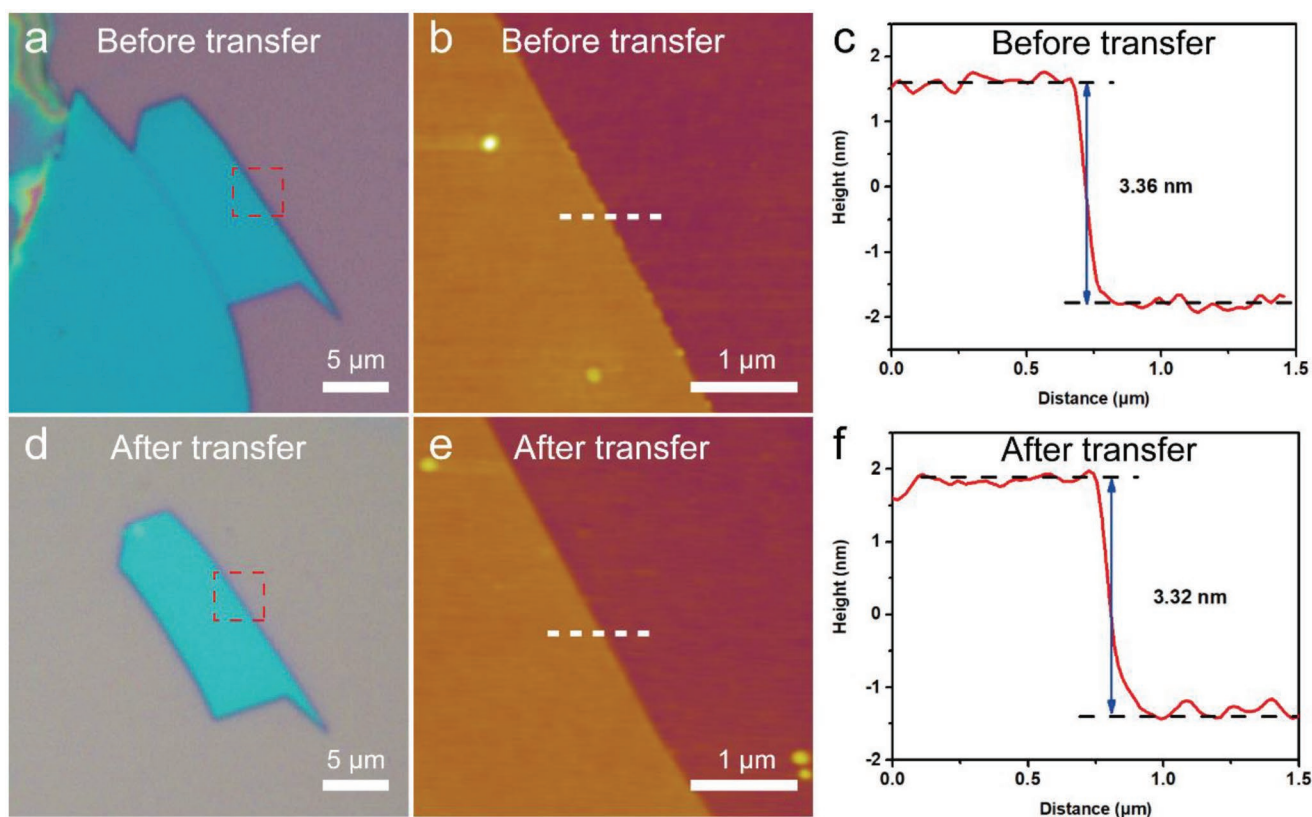


**Figure 2.** Clean transfer of MoS<sub>2</sub> from one substrate to another. a,b) Optical microscopy and AFM images of few-layer MoS<sub>2</sub> on substrate before transfer. d,e) Optical microscopy and AFM images of few-layer MoS<sub>2</sub> on substrate after transfer. c,f) Corresponding height profiles of the MoS<sub>2</sub> sample in white line before and after transfer, respectively.

is often used for the entire process of transfer (Figure S4, Supporting Information). To clearly emphasize the bond reduction effect of ethanol, a transfer with and without ethanol is recorded by a charge coupled device (CCD) camera connected to the control table (Movies S1 and S2, Supporting Information). The 2D material on a 300 nm SiO<sub>2</sub>/Si substrate is first prepared by mechanical exfoliation (Figure 1a). Notice that because the 2D material attached to the substrate surface has a high adhesion energy, it cannot be toggled or detached from the substrate with the probe, as shown in Movie S1 of the Supporting Information. The demonstration in the second recording shows the whole system of 2D material and substrate immersed in the ethanol solution. Ethanol then intercalates into the space between the 2D material and the substrate. As previously explained, the adhesion energy between 2D material and ethanol will be much smaller, enabling the probe to pry up the 2D material (Figure 1b). The 2D material can then be successfully transferred to the target substrate with the precise control of the probe (Figure 1c). Once the 2D material is placed on the targeted location, the ethanol evaporates autonomously and after annealing the whole transfer process is completed (Figure 1d). In addition to the system of ethanol and MoS<sub>2</sub>, we have also performed the successful transfer with other organic solvents such as isopropanol and acetone for MoS<sub>2</sub> and WSe<sub>2</sub> (Figure S5, Supporting Information). Considering the transfer is operated in an open environment, ethanol is still considered as the most suitable solvent for its low toxicity.

The use of ethanol is clean and free of contaminations introduced during the transfer process. The quality of 2D materials transferred by this method is carefully examined by an AFM shown in Figure 2. Mechanically exfoliated few-layer MoS<sub>2</sub> is successfully transferred from a 300 nm SiO<sub>2</sub>/Si substrate to a target one (SiO<sub>2</sub>/Si substrate). By comparing the optical microscopy images of MoS<sub>2</sub> on the original (Figure 2a) and target substrate (Figure 2d), it can be seen that the MoS<sub>2</sub> sample preserves the same shape and flatness after the transfer process. The high fidelity and ultracleaness of the sample's surface are also confirmed by AFM images (Figure 2b,e). The thicknesses of sample are 3.36 and 3.32 nm before and after the transfer (Figure 2c,f), remaining the same as shown from the height profiles of the MoS<sub>2</sub>, confirming that no residue was left on the sample. Compared with mechanically exfoliated samples, chemical vapor deposited (CVD) grown counterparts typically have stronger bonding energy between sample and growth substrate. With the assistance of ethanol, we can enable successful transfer of the CVD grown tellurium (Te) 2D nanoplates (Figure S6, Supporting Information).

This transferring method is not only clean for use in the fine assembly of 2D building blocks, but also ideal for the construction of suspended structures. Various assembled structures such as predefined patterns and van der Waals heterostructures have been demonstrated (Figures S7 and S8, Supporting Information). Figure 3a–d shows the entire process of building WSe<sub>2</sub>/MoS<sub>2</sub> heterostructures during which MoS<sub>2</sub> is transferred

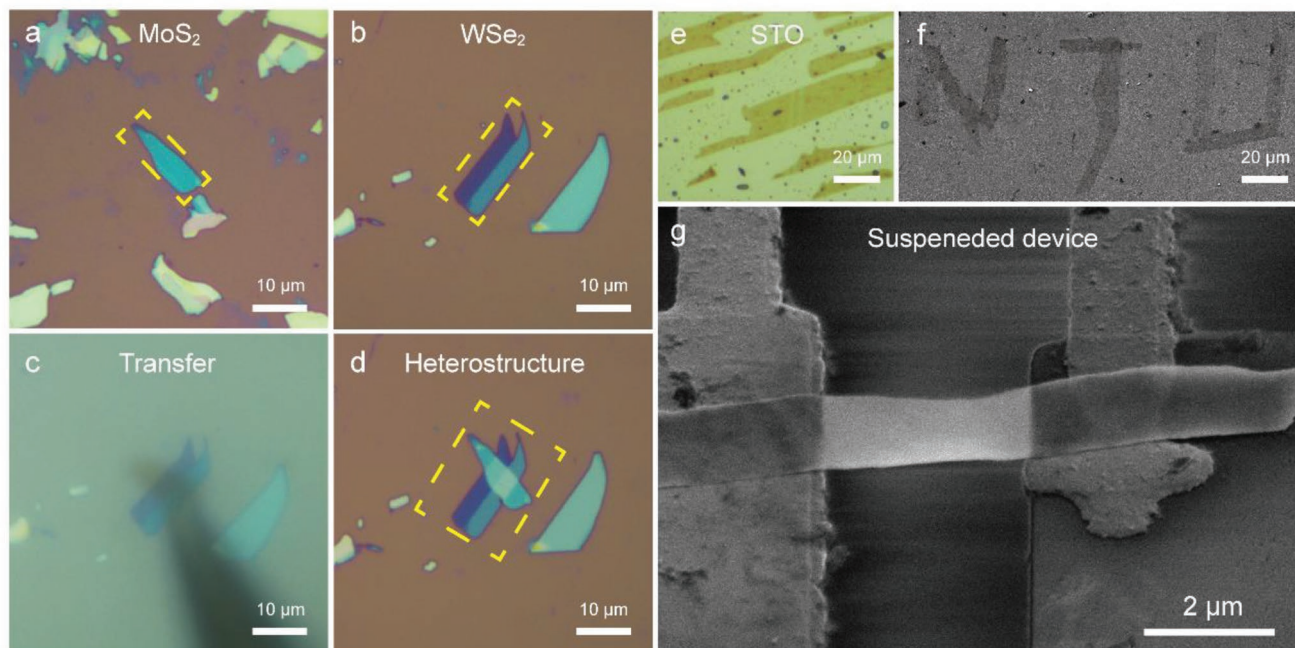


**Figure 3.** Preparation of heterostructure, predefined pattern, and suspended sample. a) MoS<sub>2</sub> on SiO<sub>2</sub>/Si substrate. b) WSe<sub>2</sub> on SiO<sub>2</sub>/Si substrate. c) Transferring MoS<sub>2</sub> immersed in ethanol to the top of WSe<sub>2</sub>. d) Laying down MoS<sub>2</sub> and drying ethanol, then a heterojunction is fabricated. e) Optical image of long strips of STO on substrate. f) SEM image of NJU initials prepared by precise control of stacking angle of STO sample. g) Transfer of STO sample on suspended device.

to sit directly on top of WSe<sub>2</sub>. The stacking angle, another important factor for 2D building blocks, can also be precisely controlled. As an example, different long strips of thin SrTiO<sub>3</sub> (STO) film (18.15 nm) can be transferred and stacked to write the letters N, J, and U (for Nanjing University), as shown in Figure 3e,f and Figure S9 (Supporting Information). To reveal the pristine properties of 2D materials with no influence from the substrate, transferring 2D materials directly onto a suspended device is of critical importance. As shown in Figure 3g, the 2D STO stripes can be positioned onto the suspended device using this transfer method. It can also be widely applied to other 2D materials like MoS<sub>2</sub> and graphene (Figure S10, Supporting Information). To find the limit of thickness for feasible transfer, we have prepared MoS<sub>2</sub> samples with different thicknesses. Just like many other transfer method, it becomes more difficult to transfer as samples become thinner, MoS<sub>2</sub> nanosheet as thin as two layer can still be successfully transferred with well-preserved quality. It is also noteworthy that there are chances that thin nanosheets can be damaged by the rough surface of needle, as shown in Figure S11 of the Supporting Information.

With different 2D building blocks on suspended devices fabricated, this new transferring method will help in the discovery of the intrinsic properties<sup>[18]</sup> of 2D materials, such as thermal properties,<sup>[19]</sup> which are directly correlated with the crystalline structure of 2D materials.<sup>[20]</sup> Previously, it has been reported that with a polymethyl methacrylate (PMMA) assisted transfer method,<sup>[21]</sup> the intrinsic properties of 2D materials suffered from significant performance degradation<sup>[22]</sup> due to polymer residues on the surface even after annealing at high temperature.<sup>[15,23]</sup> High-resolution transmission electron microscopy (TEM) confirms the good

quality of single crystal MoS<sub>2</sub> sample after transfer, as seen in Figure 4a,b. To illustrate that our transfer method is truly free of contamination or quality degradation further, we measured the thermal conductivity of a mechanically exfoliated MoS<sub>2</sub> flake after being transferred onto the suspended microbridge device. A plot showing the relationship between thermal conductivity and temperature of the five layer MoS<sub>2</sub> while using our clean transfer method is shown in Figure 4c. The inset in the graph shows an scanning electron microscopy (SEM) image of the sample on a suspended device. The plot clearly shows thermal conductivity first increasing and then decreasing with a peak at 140 K. We calculated the room-temperature thermal conductivity of this five layer MoS<sub>2</sub> using the total measured thermal resistance. Detailed analysis of the thermal contact resistance is shown in the Supporting Information and the thermal conductivity is shown in Figure S12 of the Supporting Information. The room-temperature thermal conductivity of 52 W m<sup>-1</sup> K<sup>-1</sup> is slightly higher than those in previous studies<sup>[24]</sup> measured with the same microbridge method (Figure S13, Table S4, Supporting Information), confirming that the crystal quality of the 2D material is well preserved during the transfer process. Because the intrinsic crystalline quality affects the thermal properties of MoS<sub>2</sub> flakes, it is clear from the measured results that transferring the sample with an ultraclean method is favorable for the exploration of intrinsic thermal transport properties of the MoS<sub>2</sub> sample.

### 3. Conclusion

In summary, we have demonstrated an ethanol assisted transfer (EAT) method which can enable clean assembly of 2D building

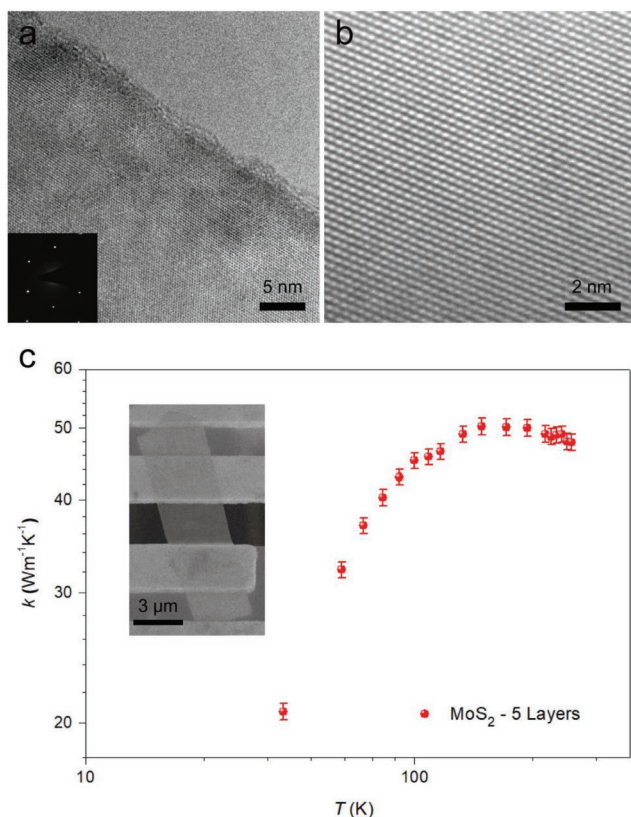


**Figure 4.** a) Transmission electron microscopy of a few-layer MoS<sub>2</sub> sample transferred onto Cu grids with ethanol. Inset: selected area electron diffraction pattern of the sample. b) High-resolution TEM image of the MoS<sub>2</sub> sample showing the good crystal quality. c) The measured thermal conductivity of MoS<sub>2</sub> by clean transfer from the original substrate onto a suspended device. Inset: an SEM image of this five layer sample.

blocks and suspended structures. MD studies and liquid AFM test reveal that ethanol can intercalate into the space between 2D materials and the substrate, weaken the adhesion energy between them and facilitate the successful detachment and transfer of the 2D materials. This transfer method is clean and does not result in any contamination to the sample, as evidenced by AFM tests. Various assembled structures such as vdWHs and predefined pattern can be built using precise positioning and arbitrary control of stacking angle, and especially can be transferred onto suspended devices. A higher room-temperature thermal conductivity of a five layer MoS<sub>2</sub> sample to be 52 W m<sup>-1</sup> K<sup>-1</sup>, confirmed that 2D materials preserve their high quality after being transferred. It can be expected that this clean, feasible, and precise EAT method can serve as a powerful tool for constructing novel materials and structures based on 2D building blocks, and exploring their intrinsic properties and functionalities onto suspended devices.

## 4. Experimental Section

**Preparation of Materials:** MoS<sub>2</sub> and WSe<sub>2</sub> flakes were prepared on clean SiO<sub>2</sub>/Si substrates by mechanically exfoliating the MoS<sub>2</sub> and WSe<sub>2</sub> crystals (XFNANO) with scotch tape (3M Scotch Tape 600). The same

preparation method was used on the graphene samples, exfoliated from highly oriented pyrolytic graphite Grade A (XFNANO). SrTiO<sub>3</sub> (STO) is prepared by etching of superfluous water-soluble layers. The first step is the epitaxial growth of water-soluble Sr<sub>3</sub>Al<sub>2</sub>O<sub>6</sub> on perovskite substrates, followed by the in situ growth of films. STO single-crystalline membranes are produced by etching the Sr<sub>3</sub>Al<sub>2</sub>O<sub>6</sub> layer in water, which are then transferred to SiO<sub>2</sub>/Si substrates.

**Characterizations:** The success of this new transfer method depends on maintaining a high degree of “cleanness” and “flatness” of the materials post transfer. These criteria were measured using an AFM. The AFM’s contact mode was used to measure the sample’s surface area and thickness (Cypher AFM, Oxford Instrument, Inc). A commercial AFM instrument (Dimension ICON with Nanoscope V controller, Bruker) was used to image the samples in air and liquid. The STO was used to write the initials “NJU” on the substrate, while the 2D materials placed on suspended devices were characterized using scanning electron microscopy (FEI Helios 600i) and transmission electron microscopy (FEI Tecnai F20).

## Supporting Information

Supporting Information is available from the Wiley Online Library or from the author.

## Acknowledgements

X.Y. and X.L. contributed equally to this work. The authors acknowledge the microfabrication center of National Laboratory of Solid State Microstructures (NLSSM) for technique support and Jiangsu Donghai Silicon Industry Science and Technology Innovation Center. This work was jointly supported by the State Key Program for Basic Research of China (No. 2015CB659300) and the National Key Research and Development Program of China (No. 2017YFA0205700), National Natural Science Foundation of China (Nos. 21805132, 11574143, 11874211, 11621091, and 61735008), National Science Foundation of Jiangsu Province (No. BK20180341), and the Fundamental Research Funds for the Central Universities (Nos. 021314380150, 021314380140). The authors thank Prof. Yuefeng Nie for providing the thin film STO samples used during the experiments. The authors thank Prof. Junjiao Wu for all the generous help regarding the thermal measurement.

## Conflict of Interest

The authors declare no conflict of interest.

## Keywords

2D, ethanol, suspended, thermal conductivity, transfer

Received: March 25, 2019

Published online:

- [1] A. Splendiani, L. Sun, Y. Zhang, T. Li, J. Kim, C. Y. Chim, G. Galli, F. Wang, *Nano Lett.* **2010**, *10*, 1271.
- [2] L. Britnell, R. Gorbachev, R. Jalil, B. Belle, F. Schedin, A. Mishchenko, T. Georgiou, M. Katsnelson, L. Eaves, S. Morozov, *Science* **2012**, *335*, 947.
- [3] a) K. Kang, S. Xie, L. Huang, Y. Han, P. Y. Huang, K. F. Mak, C.-J. Kim, D. Muller, J. Park, *Nature* **2015**, *520*, 656;

- b) B. Radisavljevic, A. Radenovic, J. Brivio, i. V. Giacometti, A. Kis, *Nat. Nanotechnol.* **2011**, *6*, 147; c) R. Cheng, J. Bai, L. Liao, H. Zhou, Y. Chen, L. Liu, Y.-C. Lin, S. Jiang, Y. Huang, X. Duan, *Proc. Natl. Acad. Sci. USA* **2012**, *109*, 11588.
- [4] a) Q. H. Wang, K. Kalantar-Zadeh, A. Kis, J. N. Coleman, M. S. Strano, *Nat. Nanotechnol.* **2012**, *7*, 699; b) H. R. Gutiérrez, N. Perea-López, A. L. Elías, A. Berkdemir, B. Wang, R. Lv, F. López-Urías, V. H. Crespi, H. Terrones, M. Terrones, *Nano Lett.* **2013**, *13*, 3447.
- [5] W. Ho, J. C. Yu, J. Lin, J. Yu, P. Li, *Langmuir* **2004**, *20*, 5865.
- [6] K. Kim, M. Yankowitz, B. Fallahzad, S. Kang, H. C. Movva, S. Huang, S. Larentis, C. M. Corbet, T. Taniguchi, K. Watanabe, S. K. Banerjee, B. J. LeRoy, E. Tutuc, *Nano Lett.* **2016**, *16*, 1989.
- [7] A. L. Elías, N. Perea-Lopez, A. Castro-Beltran, A. Berkdemir, R. Lv, S. Feng, A. D. Long, T. Hayashi, Y. A. Kim, M. Endo, *ACS Nano* **2013**, *7*, 5235.
- [8] L. Jiao, B. Fan, X. Xian, Z. Wu, J. Zhang, Z. Liu, *J. Am. Chem. Soc.* **2008**, *130*, 12612.
- [9] a) W.-H. Lin, T.-H. Chen, J.-K. Chang, J.-I. Taur, Y.-Y. Lo, W.-L. Lee, C.-S. Chang, W.-B. Su, C.-I. Wu, *ACS Nano* **2014**, *8*, 1784; b) H. Li, J. Wu, X. Huang, Z. Yin, J. Liu, H. Zhang, *ACS Nano* **2014**, *8*, 6563; c) M. Her, R. Beams, L. Novotny, *Phys. Lett. A* **2013**, *377*, 1455; d) L. Gao, G. X. Ni, Y. Liu, B. Liu, A. H. Castro Neto, K. P. Loh, *Nature* **2014**, *505*, 190; e) Y. Liu, R. Cheng, L. Liao, H. Zhou, J. Bai, G. Liu, L. Liu, Y. Huang, X. Duan, *Nat. Commun.* **2011**, *2*, 579.
- [10] a) X. Li, Y. Zhu, W. Cai, M. Borysiak, B. Han, D. Chen, R. D. Piner, L. Colombo, R. S. Ruoff, *Nano Lett.* **2009**, *9*, 4359; b) J. Kang, S. Hwang, J. H. Kim, M. H. Kim, J. Ryu, S. J. Seo, B. H. Hong, M. K. Kim, J.-B. Choi, *ACS Nano* **2012**, *6*, 5360.
- [11] a) M. A. Meitl, Z.-T. Zhu, V. Kumar, K. J. Lee, X. Feng, Y. Y. Huang, I. Adesida, R. G. Nuzzo, J. A. Rogers, *Nat. Mater.* **2006**, *5*, 33; b) Y. H. Lee, L. Yu, H. Wang, W. Fang, X. Ling, Y. Shi, C. T. Lin, J. K. Huang, M. T. Chang, C. S. Chang, M. Dresselhaus, T. Palacios, L. J. Li, J. Kong, *Nano Lett.* **2013**, *13*, 1852.
- [12] S. J. Kim, T. Choi, B. Lee, S. Lee, K. Choi, J. B. Park, J. M. Yoo, Y. S. Choi, J. Ryu, P. Kim, J. Hone, B. H. Hong, *Nano Lett.* **2015**, *15*, 3236.
- [13] a) A. Gurarslan, Y. Yu, L. Su, Y. Yu, F. Suarez, S. Yao, Y. Zhu, M. Ozturk, Y. Zhang, L. Cao, *ACS Nano* **2014**, *8*, 11522; b) B. Li, Y. He, S. Lei, S. Najmaei, Y. Gong, X. Wang, J. Zhang, L. Ma, Y. Yang, S. Hong, J. Hao, G. Shi, A. George, K. Keyshar, X. Zhang, P. Dong, L. Ge, R. Vajtai, J. Lou, Y. J. Jung, P. M. Ajayan, *Nano Lett.* **2015**, *15*, 5089.
- [14] G. F. Schneider, V. E. Calado, H. Zandbergen, L. M. Vandersypen, C. Dekker, *Nano Lett.* **2010**, *10*, 1912.
- [15] I. Jo, M. T. Pettes, J. Kim, K. Watanabe, T. Taniguchi, Z. Yao, L. Shi, *Nano Lett.* **2013**, *13*, 550.
- [16] C. Wang, J. Guo, L. Dong, A. Aiyiti, X. Xu, B. Li, *Sci. Rep.* **2016**, *6*, 25334.
- [17] Q. Jiang, H. M. Lu, *Surf. Sci. Rep.* **2008**, *63*, 427.
- [18] Y. Wang, N. Xu, D. Li, J. Zhu, *Adv. Funct. Mater.* **2017**, *27*, 1604134.
- [19] X. Li, Y. Liu, Q. Zheng, X. Yan, X. Yang, G. Lv, N. Xu, Y. Wang, M. Lu, K. Chen, J. Zhu, *Appl. Phys. Lett.* **2017**, *111*, 163102.
- [20] D.-W. Oh, J. Ravichandran, C.-W. Liang, W. Siemons, B. Jalan, C. M. Brooks, M. Huijben, D. G. Schlom, S. Stemmer, L. W. Martin, *Appl. Phys. Lett.* **2011**, *98*, 221904.
- [21] a) L. Shi, D. Li, C. Yu, W. Jang, D. Kim, Z. Yao, P. Kim, A. Majumdar, *J. Heat Transfer* **2003**, *125*, 881; b) A. Weathers, L. Shi, *Annu. Rev. Heat Transfer* **2013**, *16*, 101.
- [22] J. W. Suk, W. H. Lee, J. Lee, H. Chou, R. D. Piner, Y. Hao, D. Akinwande, R. S. Ruoff, *Nano Lett.* **2013**, *13*, 1462.
- [23] M. T. Pettes, I. Jo, Z. Yao, L. Shi, *Nano Lett.* **2011**, *11*, 1195.
- [24] a) I. Jo, M. T. Pettes, E. Ou, W. Wu, L. Shi, *Appl. Phys. Lett.* **2014**, *104*, 201902; b) A. Aiyiti, S. Hu, C. Wang, Q. Xi, Z. Cheng, M. Xia, Y. Ma, J. Wu, J. Guo, Q. Wang, J. Zhou, J. Chen, X. Xu, B. Li, *Nanoscale* **2018**, *10*, 2727.